

MODELING OF THE HAZE-PRODUCING SECONDARY POLLUTANT CONCENTRATIONS IN THE ATMOSPHERE

UDC 504.3.054:551.575.1 535.247:539.175

L.A. Jimoda¹, J.A. Sonibare², F.A. Akeredolu²

¹Department of Chemical Engineering, Ladoké Akintola University of Technology, Ogbomoso, Nigeria

²Department of Chemical Engineering, Obafemi Awolowo University, Ile-Ife, Nigeria

Abstract. *In this work we have developed a model for predicting the rate of formation of secondary pollutants in the atmosphere. Haze-producing secondary pollutants including peroxyacetyl nitrate (PAN), Ozone (O₃), Nitrate (NO₃⁻) and Sulphate (SO₄²⁻) were modeled by determining the rate equation balance for each component. The photochemical chain reaction mechanisms producing the desired secondary pollutants were used to obtain the required rate equation balance so as to set up the resultant first order differential equations. The rate constants for the chosen plug flow reactions were estimated. The initial concentrations of each component in the reactor and rate constants obtained were used in a set of first order differential equations to validate the concentrations of (PAN, NO₃⁻, SO₄²⁻, O₃). Six-hour samplings in each quarter of a year were carried out for a period of 24 hours to validate the concentrations of secondary pollutants (PAN, HNO₃, H₂SO₄, O₃). The ordinary differential equation (ODE) solver of MATLAB 8.0 was used to determine the concentration profiles of the secondary pollutants with a time increment of 1 hour for a period of 24 hours. The result of the reactor modeling showed that peroxyacetyl nitrate (PAN) and NO₃⁻ concentrations reduced with sunlight but increased with rainfall while Ozone (O₃) and Sulphate (SO₄²⁻) concentrations increased with sunlight and reduced with rainfall. The developed model results confirmed the variation of the concentration of secondary pollutants with sunlight and rainfall.*

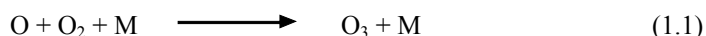
Key words: *haze-producing, secondary pollutants, photochemical reaction, chain reaction*

1. INTRODUCTION

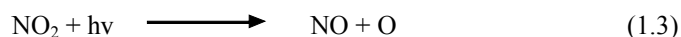
Transformations of the primary air pollutants in the atmosphere usually produce secondary air pollutants. The chemical transformations are best characterized as oxidation processes. The oxygenated species are the secondary products which are formed in the atmosphere from the primary emissions of anthropogenic or natural sources (Pitts *et al.*,

1977). During photochemical reactions, photons interact with other species, which eventually results in the formation of products. These can occur in the form of gas (homogeneous reactions), on a surface or in a liquid droplet (heterogeneous reactions). In this study, chemical transformations that occur in a gas phase producing secondary products such as nitrate (NO_3^-), sulphate (SO_4^{2-}), O_3 and Peroxylacetyl nitrate (PAN) are studied.

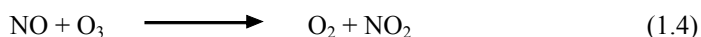
Ozone in the atmosphere originates from major sources, including the stratosphere, the free troposphere, and through boundary layer photochemical reactions (Derwent and Kay, 1988). The formation pathway generally follows:



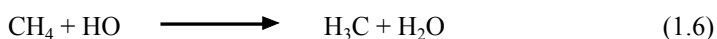
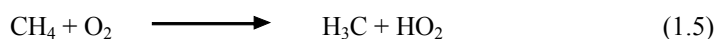
M is a molecule of nitrogen (N_2) or Oxygen (O_2) whose participation is necessary to conserve energy and momentum. N_2 and O_2 react at high temperatures of about 1210-1765°C which are usually attained in the combustion process involving air forming nitrogen oxide (NO).



Sunlight in the day tends to favour reactions producing NO and O, hence increasing ozone concentration. The presence of volatile organic compounds (VOCs) in the atmosphere prevents the ozone formed from being immediately consumed by NO to produce NO_2 (Curtics and Rabl, 1996) as:



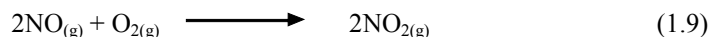
Organic compounds, especially the VOCs, are more likely to lead the aerosol formation by their general high reactivity and types of oxidation products (Sonibare, 2009). Such VOCs absorb solar radiation and undergo various photochemical and chemical reactions involving free radicals and intermediates, forming final products that contribute to photochemical smog in the atmosphere. Some of these reactions are catalysed by particulate matter such as soot and metal oxides. The formation mechanisms that produced H_3COO radicals in the formation of PAN were summarized by Dara (2006) as:



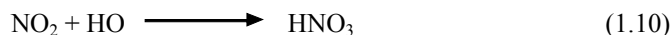
The secondary particulate nitrate in the form of HNO_3 is formed as a result of atmospheric reactions of NO/ NO_2 involving gas to particle conversion (Michalsk *et al.*, 2004). During thunderstorms or lightning, NO is formed from an interaction between N_2 and O_2 :



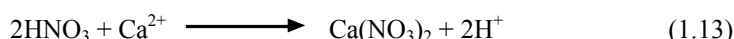
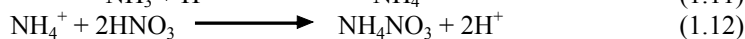
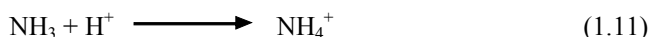
The same reaction occurs in the internal combustion engines of automobiles because of the presence of nitrogen in the fuel which reacts with oxygen forming NO that is released through the exhaust pipe. NO is also released through other combustion sources which include aircrafts, refineries and biomass burning. However, for NO_2 formation, NO is photochemically oxidized through its major sources, which include fossil fuel combustion, biomass burning and wood burning from the reaction:



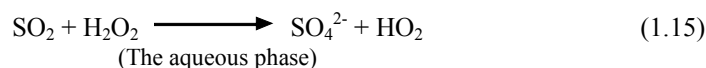
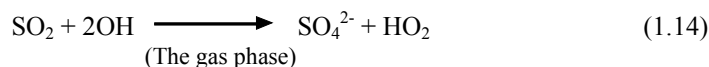
Summarily, in the stratosphere, NO_2 may react with the HO free radical forming HNO_3 as:



The produced HNO_3 is removed as acid rain or it is converted into particulate nitrate due to neutralization by ammonia (NH_3) or particulate lime.



Sulphate (SO_4^{2-}) as H_2SO_4 secondary aerosol is principally formed from the atmospheric conversion of SO_2 produced as a product of fossil fuel combustion processes among other. Air pollution due to SO_2 is the result of coal burning and combustion of petroleum products. Metallurgical operations such as smelting (mostly Cu and Zn) contribute substantially to the amount of SO_2 in the atmosphere. Generally, H_2SO_4 often results from photochemical oxidation reactions or the oxidation of atmospheric SO_2 if a catalyst (MnSO_4 or some metal oxides) is present (Dara, 2006). The formation of H_2SO_4 in the atmosphere formation is usually found either in the gas or aqueous phases with hydroxyl or hydroperoxyl radicals as important reacting agents (Stein and Lamb, 2003). However, the aqueous phase of oxidation is the predominant mechanism for sulphate formation under fog conditions (Lazaridis and Skouloudis, 1999).



Weber *et al.* (1997) simultaneously measured aerosol particles and their expected gas phase precursors in the atmosphere. New particle formation due to the formation of H_2SO_4 as a secondary pollutant was identified by the presence of ultra fine particle concentrations in a diurnal pattern. This was attributed to the photochemical production of the precursor species. De More *et al.* (1992) estimated the rate at which H_2SO_4 vapour is produced using:

$$R = k [\text{OH}] [\text{SO}_2] \quad (1.16)$$

The rate constant k was found to be dependent on ambient temperature and pressure with a range of $7-9 \times 10^{-13} \text{ cm}^3\text{s}^{-1}$. However, H_2SO_4 concentration is likely to be in a steady state balance between production and loss whenever H_2SO_4 scavenging rates are high in the plumes.

Weber *et al.* (2007) studied the formation of secondary organic aerosol (SOA) in an anthropogenic-influenced region in the Southeastern United States measuring water soluble organic carbon (WSOC) in the fine particles as a measure of secondary organic aerosol in the area. A comparison was made between SOA formations in plumes advected from New York City. Measurements of biogenic VOCs showed that the Atlanta/North Georgia region contained on average 10-100 times higher concentrations compared with

the one that was advected from New York City. The results showed that anthropogenic components which are higher in the Southeastern United States play a role in the formation of SOA in the area.

Sullivan *et al.* (2004) used online continuous measurement for measuring water-soluble organic compound (WSOC) components of aerosol particles in St. Louis. A particle to liquid sampler was used to collect the ambient particles that later washed into a flow of purified water. The resulting liquid was then filtered so as to determine the carbon content level that was quantified using a Total Organic Carbon Analyzer. The measurement showed that WSOC and OC described as WSOC/OC ranged between 0.40 and 0.80. The measurements carried out in June and August were observed to differ significantly due to a number of factors including atmospheric chemical and meteorological processes and emissions.

Peltier *et al.* (2007) modified and coupled a particle-into liquid sampler (PILS) with a total organic carbon (TOC) analyzer for the measurement of particulate organic carbon. The PILS-OC technique was deployed in Atlanta Georgia and Riverside California to measure ambient aerosol carbon in the area. The PILS droplet collection system was changed from an inertia impactor to a miniature cyclone to increase the efficiency of transferring insoluble carbonaceous aerosol to the liquid sample stream.

Hennigan *et al.* (2008) measured atmospheric gases and fine particle chemistry of the Mexico City Metropolitan Area (MCMA) at a site about 30 km downwind of the city center. The work showed that ammonium nitrate (NH_4NO_3) dominated the inorganic aerosol fraction. In addition, NO_3^- and WSOC were found to be highly correlated during the morning and early afternoon hours when concentrations of these species grew quickly. The volatilization of secondarily-formed NO_3^- and WSOC contributed to the loss of about 25% of the secondary products.

Sillman and He (2002) proposed a result focused on a pollutant ratio such as O_3/NO_y and $\text{H}_2\text{O}_2/\text{HNO}_3$ as indicators of O_3 - NO_x -VOC sensitivity. These ratios were found to correlate with predicted NO_x -VOC sensitivity for a variety of zero-dimensional and three-dimensional models. These models were found to be significant in designing a control strategy that reduces the two main precursors of ozone concentrations in the atmosphere (NO_x and VOC). These correlations with NO_x -VOC sensitivity were found to be stronger and more consistent for ratios involving peroxides ($\text{H}_2\text{O}_2/\text{HNO}_3$) than other ratios such as O_3/NO_2 .

2. MATERIALS AND METHODS

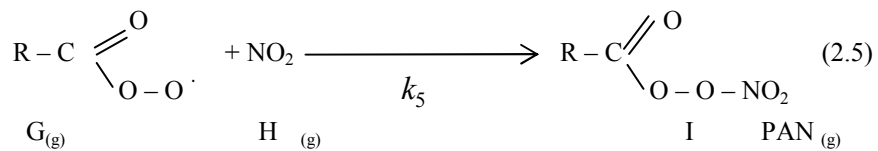
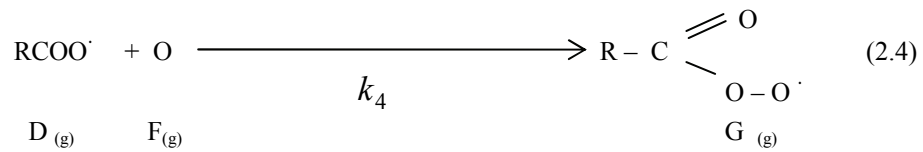
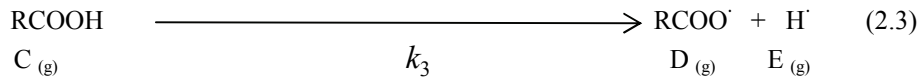
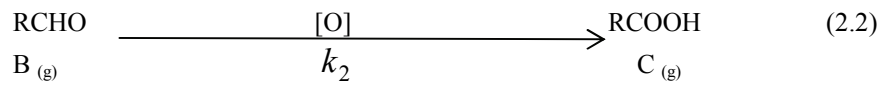
The reactor modeling steps for formation of gas phase secondary pollutants (PAN, O_3 , NO_3^- and SO_4^{2-}) in the atmosphere as carried out in the study include:

- i. Simulating the atmosphere as a chemical reactor;
- ii. Getting the photochemical chain reaction mechanisms that produce the pollutants of interest, in the reactor;
- iii. Determining the rate equation balance for each component in the reactor. This rate equation balance was used to set up the resultant first order differential equations (Froment and Bischoff, 1990).

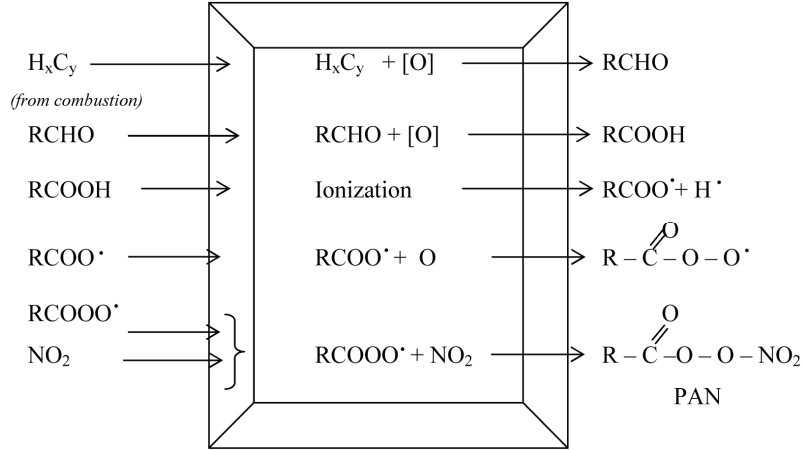
- iv. Choosing the appropriate reactor for the system and hence determining the rate constants (which depend on the chosen reactor). The reactor chosen for the system is a plug flow reactor which is characterized by gas phase reactions, reactions of constant velocity and also negligible boundary layer formation with reactor walls (Massey, 2003). The estimated rate constants were limited to zero, first and second orders since the gas phase reactions are rarely third order or greater order reactions (Wilson, 2004);
- v. The initial concentration of each of the components in the reactor and the calculated rate constants (which depend on the chosen reactor) were substituted into the first order differential equations to simulate the concentration of each component in the reactor.
- vi. The ordinary differential equation (ODE) solver of MATLAB was used to determine the concentration profiles with a time increment of 1 hour for a period of 24hours.

2.1 Atmospheric Formation of Peroxyacetyl nitrate (PAN)

Henry and Heinke (2004), Dara (2006) and Rao (2006) gave the reaction mechanisms that produce Peroxyacetyl nitrate (PAN) as:



Where k_1, k_2, k_3, k_4 and k_5 are the rate constants for each of the reactions.



The rate equation balances for the components (H_xC_y , $RCHO$, $RCOOH$, $RCOO'$, H' , O , $RCOOO'$, NO_2 and $RCOOONO_2$) are:

$$-r_{H_xC_y} = k_1[H_xC_y] \quad (2.6)$$

$$-r_{RCHO} = k_2[RCHO] - k_1[H_xC_y] \quad (2.7)$$

$$-r_{RCOOH} = k_3[RCOOH] - k_2[RCHO] \quad (2.8)$$

$$-r_{RCOO'} = k_4[RCOO'][O] - k_3[RCOOH] \quad (2.9)$$

$$r_{H'} = k_3[RCOOH] \quad (2.10)$$

$$-r_O = k_4[RCOO'][O] \quad (2.11)$$

$$-r_{RCOOO'} = k_5[RCOOO'][NO_2] - k_4[RCOO'][O] \quad (2.12)$$

$$-r_{NO_2} = k_5[RCOOO'][NO_2] \quad (2.13)$$

$$r_{PAN} = k_5[RCOOO'][NO_2] \quad (2.14)$$

The concentration of the components (H_xC_y , $RCHO$, $RCOOH$, $RCOO'$, H' , O , $RCOOO'$, NO_2 and $RCOOONO_2$) represented as A,B,C,D,E,F,G,H,I are:

$$-r_A = -\frac{d}{dt}C_A = k_1C_A \quad (2.15)$$

$$-r_B = -\frac{d}{dt}C_B = k_2C_B - k_1C_A \quad (2.16)$$

$$-r_C = -\frac{d}{dt}C_C = k_3C_C - k_2C_B \quad (2.17)$$

$$r_D = \frac{d}{dt}C_D = k_4C_D C_F - k_3C_C \quad (2.18)$$

$$r_E = \frac{d}{dt} C_E = k_3 C_C \quad (2.19)$$

$$-r_F = -\frac{d}{dt} C_F = k_4 C_D C_F \quad (2.20)$$

$$-r_G = \frac{d}{dt} C_G = k_5 C_G C_H - k_4 C_D C_F \quad (2.21)$$

$$-r_H = -\frac{d}{dt} C_H = k_5 C_G C_H \quad (2.22)$$

$$-r_I = \frac{d}{dt} C_I = k_5 C_G C_H \quad (2.23)$$

Let $C_A = x_1, C_B = x_2, C_C = x_3, C_D = x_4, C_E = x_5, C_F = x_6, C_G = x_7, C_H = x_8, C_I = x_9$

$$\frac{d}{dt} x_1 = -k_1 x_1 \quad (2.24)$$

$$\frac{d}{dt} x_2 = -[k_2 x_2 - k_1 x_1] \quad (2.25)$$

$$\frac{d}{dt} x_3 = k_3 x_3 - k_2 x_2 \quad (2.26)$$

$$\frac{d}{dt} x_4 = -[k_4 x_4 x_6 - k_3 x_3] \quad (2.27)$$

$$\frac{d}{dt} x_5 = k_3 x_3 \quad (2.28)$$

$$\frac{d}{dt} x_6 = -k_4 x_4 x_6 \quad (2.29)$$

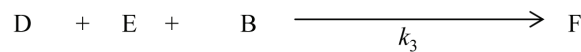
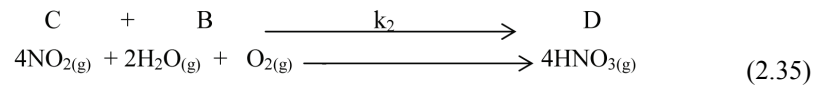
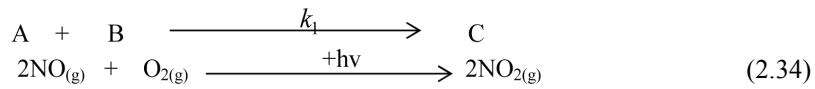
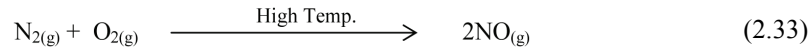
$$\frac{d}{dt} x_7 = -[k_5 x_7 x_8 - k_4 x_4 x_6] \quad (2.30)$$

$$\frac{d}{dt} x_8 = -k_5 x_7 x_8 \quad (2.31)$$

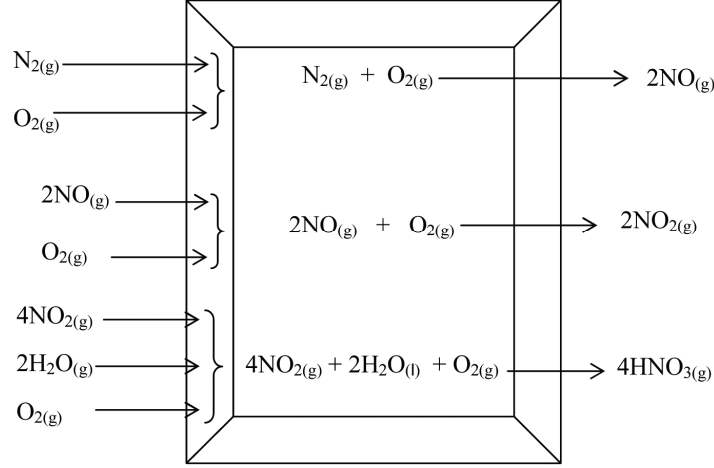
$$\frac{d}{dt} x_9 = k_5 x_7 x_8 \quad (2.32)$$

2.2 Atmospheric Formation of HNO₃

Like PAN, the reaction mechanisms that produce HNO_{3(g)} include:



The rate equation balances for the components (N_2 , O_2 , NO , NO_2 , H_2O and HNO_3) are represented as:



$$-r_{N_2} = \frac{-d[N_2]}{dt} = k_1[N_2][O_2] \quad (2.36)$$

$$(-r_{O_2})_{net} = \frac{-d[O_2]}{dt} = k_1[N_2][O_2] + k_2[NO]^2[O_2] + k_3[NO_2]^4[H_2O]^2[O_2] \quad (2.37)$$

$$-r_{NO} = \frac{-d[NO]}{dt} = k_2[NO]^2[O_2] - k_1[N_2][O_2] \quad (2.38)$$

$$-r_{NO_2} = \frac{d[NO_2]}{dt} = k_3[NO_2]^4[H_2O]^2[O_2] - k_2[NO]^2[O_2] \quad (2.39)$$

$$-r_{H_2O} = \frac{-d[H_2O]}{dt} = k_3[NO_2]^4[H_2O]^2[O_2] \quad (2.40)$$

$$r_F = \frac{d[HNO_3]}{dt} = k_3[NO_2]^4[H_2O]^2[O_2] \quad (2.41)$$

i.e.

$$-r_A = \frac{-dC_A}{dt} = k_1C_A C_B \quad (2.42)$$

$$(-r_B)_{net} = \frac{-dC_B}{dt} = k_1C_A C_B + k_2C_C^2 C_B + k_3C_D^4 C_E^2 C_B \quad (2.43)$$

$$-r_C = \frac{-dC_C}{dt} = k_2C_C^2 C_B - k_1C_A C_B \quad (2.44)$$

$$-r_D = \frac{-dC_D}{dt} = k_3C_D^4 C_E^2 C_B - k_2C_C^2 C_B \quad (2.45)$$

$$-r_E = \frac{-dC_E}{dt} = k_3C_D^4 C_E^2 C_B \quad (2.46)$$

$$r_F = \frac{dC_F}{dt} = k_3C_D^4 C_E^2 C_B \quad (2.47)$$

The equations above can be summarized as:

$$\frac{d}{dt} C_A = -k_1 C_A C_B \quad (2.48)$$

$$\frac{d}{dt} C_B = -(k_1 C_A C_B + k_2 C_C^2 C_B + k_3 C_D^4 C_E^2 C_B) \quad (2.49)$$

$$\frac{d}{dt} C_C = k_1 C_A C_B - k_2 C_C^2 C_B \quad (2.50)$$

$$\frac{d}{dt} C_D = k_2 C_C^2 C_B - k_3 C_D^4 C_E^2 C_B \quad (2.51)$$

$$\frac{d}{dt} C_E = -k_3 C_D^4 C_E^2 C_B \quad (2.52)$$

$$\frac{d}{dt} C_F = k_3 C_D^4 C_E^2 C_B \quad (2.53)$$

Let $C_A = x_1, C_B = x_2, C_C = x_3, C_D = x_4, C_E = x_5$, and $C_F = x_6 \Rightarrow$

$$\frac{d}{dt} x_1 = -k_1 x_1 x_2 \quad (2.54)$$

$$\frac{d}{dt} x_2 = -(k_1 x_1 x_2 + k_2 x_3^2 x_2 + k_3 x_4^4 x_5^2 x_2) \quad (2.55)$$

$$\frac{d}{dt} x_3 = k_1 x_1 x_2 - k_2 x_3^2 x_2 \quad (2.56)$$

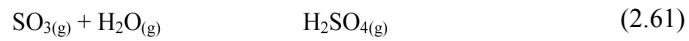
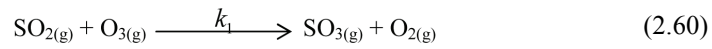
$$\frac{d}{dt} x_4 = k_2 x_3^2 x_2 - k_3 x_4^4 x_5^2 x_2 \quad (2.57)$$

$$\frac{d}{dt} x_5 = -k_3 x_4^4 x_5^2 x_2 \quad (2.58)$$

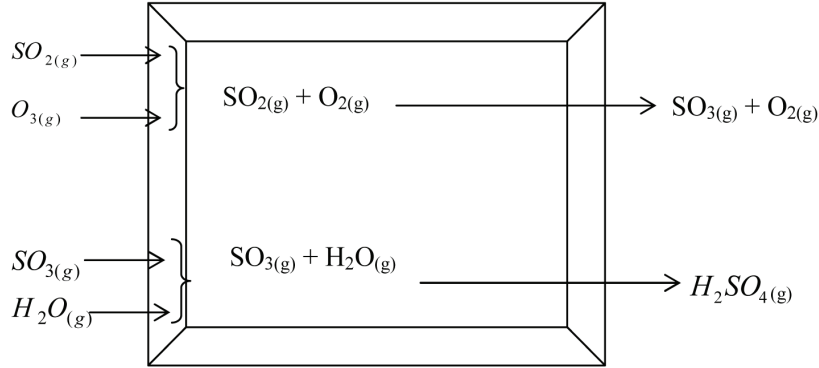
$$\frac{d}{dt} x_6 = k_3 x_4^4 x_5^2 x_2 \quad (2.59)$$

2.3 Atmospheric Formation of H₂SO₄

In the atmosphere, several reaction mechanisms that produce H₂SO₄(g) are shown below:



Where k_1 and k_2 are rate constants for each of the reactions.



The rate equation balances for the components SO_2 , O_3 , SO_3 , O_2 , H_2O and H_2SO_4 are represented as:

$$-r_{SO_2} = \frac{-d[SO_2]}{dt} = k_1[SO_2][O_3] \quad (2.62)$$

$$-r_{O_3} = \frac{-d[O_3]}{dt} = k_1[SO_2][O_3] \quad (2.63)$$

$$(-r_{SO_3})_{net} = \frac{-d[SO_3]}{dt} = k_2[SO_3][H_2O] - k_1[SO_2][O_3] \quad (2.64)$$

$$r_{O_2} = \frac{d[O_2]}{dt} = k_1[SO_2][O_3] \quad (2.65)$$

$$-r_{H_2O} = \frac{-d[H_2O]}{dt} = k_2[SO_3][H_2O] \quad (2.66)$$

$$r_{H_2SO_4} = \frac{d[H_2SO_4]}{dt} = k_2[SO_3][H_2O] \quad (2.67)$$

The concentrations of the components (SO_2 , O_3 , SO_3 , O_2 , H_2O and H_2SO_4) are represented as C_A , C_B , C_C , C_D , C_E and C_F as shown below:

$$-r_A = \frac{-dC_A}{dt} = k_1 C_A C_B \quad (2.68)$$

$$-r_B = \frac{-dC_B}{dt} = k_1 C_A C_B \quad (2.69)$$

$$-r_C = \frac{-dC_C}{dt} = k_2 C_C C_E - k_1 C_A C_B \quad (2.70)$$

$$r_D = \frac{dC_D}{dt} = k_1 C_A C_B \quad (2.71)$$

$$-r_E = \frac{-dC_E}{dt} = k_2 C_C C_E \quad (2.72)$$

$$r_F = \frac{dC_F}{dt} = k_2 C_C C_E \quad (2.73)$$

The equations above can be summarized as:

$$\frac{d}{dt} C_A = -k_1 C_A C_B \quad (2.74)$$

$$\frac{d}{dt} C_B = -k_1 C_A C_B \quad (2.75)$$

$$\frac{d}{dt} C_C = -(k_2 C_C C_E - k_1 C_A C_B) \quad (2.76)$$

$$\frac{d}{dt} C_D = k_1 C_A C_B \quad (2.77)$$

$$\frac{d}{dt} C_E = -k_2 C_C C_E \quad (2.78)$$

$$\frac{d}{dt} C_F = k_2 C_C C_E \quad (2.79)$$

Let $C_A = x_1, C_B = x_2, C_C = x_3, C_D = x_4, C_E = x_5$ and $C_F = x_6 \Rightarrow$

$$\frac{d}{dt} x_1 = -k_1 x_1 x_2 \quad (2.80)$$

$$\frac{d}{dt} x_2 = -k_1 x_1 x_2 \quad (2.81)$$

$$\frac{d}{dt} x_3 = -(k_2 x_3 x_5 - k_1 x_1 x_2) \quad (2.82)$$

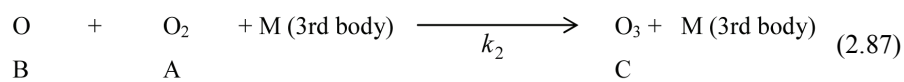
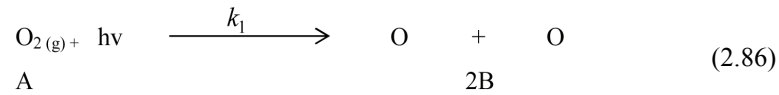
$$\frac{d}{dt} x_4 = k_1 x_1 x_2 \quad (2.83)$$

$$\frac{d}{dt} x_5 = -k_2 x_3 x_5 \quad (2.84)$$

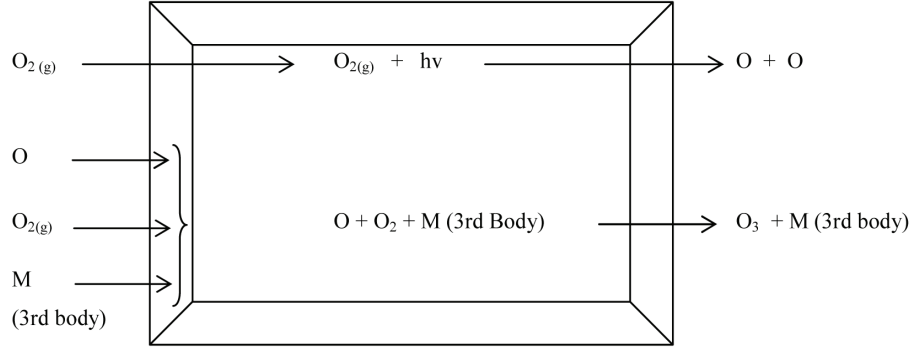
$$\frac{d}{dt} x_6 = k_2 x_3 x_5 \quad (2.85)$$

2.4 Atmospheric formation of O₃

The reaction mechanisms that produce O_{3(g)} are given as:



Where k_1 and k_2 are rate constants for the reactions.



The rate equation balances for the components (O_2 , O and O_3) are represented below:

$$-r_{O_2} = k_1[O_2] + k_2[O][O_2] \quad (2.88)$$

$$-r_O = k_2[O][O_2] + k_1[O]^2 \quad (2.89)$$

$$r_{O_3} = k_2[O][O_2] \quad (2.90)$$

i.e

$$-r_A = k_1 C_A + k_2 C_B C_A \quad (2.91)$$

$$-r_B = k_2 C_B C_A + k_1 C_B^2 \quad (2.92)$$

$$r_C = k_2 C_B C_A \quad (2.93)$$

The equations can be summarized as:

$$\frac{d}{dt} C_A = -(k_1 C_A + k_2 C_B C_A) \quad (2.94)$$

$$\frac{d}{dt} C_B = -(k_1 C_B C_A + k_1 C_B^2) \quad (2.95)$$

$$\frac{d}{dt} C_C = k_2 C_B C_A \quad (2.96)$$

Let $C_A = x_1$, $C_B = x_2$, $C_C = x_3$

$$\frac{d}{dt} x_1 = -(k_1 x_1 + k_2 x_2 x_1) \quad (2.97)$$

$$\frac{d}{dt} x_2 = -(k_1 x_2 x_1 + k_1 x_2^2) \quad (2.98)$$

$$\frac{d}{dt} x_3 = k_2 x_2 x_1 \quad (2.99)$$

3. RESULTS

The results of the ordinary differential equation solver of MATLAB 8.0 and that of measured values for each of the secondary pollutants (PAN, NO_3^- , SO_4^{2-} and O_3) during the wet season (July, 2008; May, 2009) and dry season (October, 2008; February, 2009) are shown in Tables 1 – 4:

3.1 Peroxyacetyl nitrate (PAN)

Table 1 gives the resultant predicted daily concentrations in the wet and dry seasons. The concentration of PAN decreased by about 10 - 15 % in the early morning to 12 noon in the wet season with a maximum concentration of $60.87 \mu\text{g}/\text{m}^3$ and $52.44 \mu\text{g}/\text{m}^3$ at 6.00 am (time 0 min) in July, 2008 and May, 2009 respectively. From morning to early afternoon, to evening and finally to dawn, the concentration of PAN decreased. The concentrations of PAN were $23.02 \mu\text{g}/\text{m}^3$ and $21.39 \mu\text{g}/\text{m}^3$ in July, 2008 and May, 2009 at 5.00 am (1380 min).

In the dry season, the initial concentrations of PAN in October, 2008 and February, 2009 were $47.21 \mu\text{g}/\text{m}^3$ and $43.32 \mu\text{g}/\text{m}^3$ respectively. The concentration of PAN decreased by about 15 – 30 % in the early morning to 12 noon in the dry season with maximum concentrations of $47.21 \mu\text{g}/\text{m}^3$ and $43.32 \mu\text{g}/\text{m}^3$ at 6.00 am (time 0 min) in October, 2008 and February, 2009 respectively. The PAN concentration decreased from morning to early afternoon, to evening and to dawn. The minimum concentrations of PAN were $23.72 \mu\text{g}/\text{m}^3$ and $7.24 \mu\text{g}/\text{m}^3$ in July, 2008 and May, 2009 at 5.00 am (time 1380 min).

3.2 NO_3^-

Table 2 which gave the predicted daily concentrations of NO_3^- during the two seasons revealed that there was a decrease in the concentrations of NO_3^- by about 23 – 25 % from early morning (around 6.00 am) to 12 noon during the wet season (July, 2008 and May, 2009). The maximum concentrations were obtained at dawn (around 6.00 am) with NO_3^- concentrations obtained as $20.24 \mu\text{g}/\text{m}^3$ in July, 2008 and $18.26 \mu\text{g}/\text{m}^3$ in May, 2009. The concentrations witnessed a general decrease until they reached $5.37 \mu\text{g}/\text{m}^3$ and $9.57 \mu\text{g}/\text{m}^3$ at 5 am (1380 min) in July, 2008 and May, 2009 respectively.

In the dry season, the initial concentrations of NO_3^- in October, 2008 and February, 2009 were $14.11 \mu\text{g}/\text{m}^3$ and $12.16 \mu\text{g}/\text{m}^3$ respectively. These NO_3^- concentrations decreased by about 14 – 22 % at 12 noon. This decrease of NO_3^- concentrations continued until the concentrations reached the lowest values of $5.97 \mu\text{g}/\text{m}^3$ and $7.66 \mu\text{g}/\text{m}^3$ at 5 am (1380 min) in October, 2008 and February, 2009 respectively. The NO_3^- concentrations during the day were observed to be higher than those at night.

3.3 SO_4^{2-}

The predicted daily concentrations of SO_4^{2-} as presented in Table 3 showed a different pattern to PAN and NO_3^- . During the wet season, the concentration of SO_4^{2-} increased by about 300 % after 6 hours (12 noon) when compared to the concentrations at 6.00 am. At 6.00 pm, the SO_4^{2-} concentrations decreased tremendously to about 20 % of their values at 12 noon.

At 5.00 am, SO_4^{2-} concentrations reduced to $3.02 \mu\text{g}/\text{m}^3$ in July, 2008 and $1.86 \mu\text{g}/\text{m}^3$ in May, 2009.

During the dry season, the concentrations of SO_4^{2-} increased by about 250 – 300 % after 6 hours (12 noon) when compared to the concentrations at 6.00 am. At 6.00 pm, the SO_4^{2-} concentrations decreased tremendously to about 20 – 25 % of the values at 12 noon.

At 5.00 am (1380 min), SO_4^{2-} concentrations reduced to $1.86 \mu\text{g}/\text{m}^3$ in October, 2008 and $3.02 \mu\text{g}/\text{m}^3$ in February, 2009.

3.4 O_3

The predicted O_3 concentrations as presented in Table 4 followed the same pattern as the SO_4^{2-} concentration. During the wet season, the concentration of O_3 increased by about 400 % after 6 hours (12 noon) when compared with the concentration at 6.00 am. At 6.00 pm, the O_3 concentration then decreased to about 25 % of its values at 12 noon. At 5.00 am (1380 min), O_3 concentrations reduced to $0.73 \mu\text{g}/\text{m}^3$ in July, 2008 and $0.86 \mu\text{g}/\text{m}^3$ in May, 2009.

During the dry season, the concentration of O_3 increased by about 300 – 400 % after 6 hours (12 noon) when compared with the concentrations at 6.00 am. At 6.00 pm, the O_3 concentration then decreased tremendously to about 20 – 25 % of the values at 12 noon. At 5.00 am (1380 min), O_3 concentrations reduced to $0.98 \mu\text{g}/\text{m}^3$ in October, 2008 and $1.43 \mu\text{g}/\text{m}^3$ in February, 2009.

Table 1. Predicted daily concentrations of PAN during the wet and dry seasons.

t (min.)		PAN Concentration ($\mu\text{g}/\text{m}^3$)			
		Wet Season 1 st Run	Wet Season 2 nd run	Dry Season 1 st Run	Dry Season 2 nd Run
6 am	0	60.87	52.44	47.21	43.32
7 am	60	60.21	50.37	46.20	41.24
8 am	120	58.29	48.79	45.21	39.03
9 am	180	56.24	48.62	44.23	35.76
10 am	240	55.36	48.02	43.21	34.12
11 am	300	52.37	47.92	42.26	32.22
12 noon	360	50.01	47.39	40.19	30.83
1 pm	420	49.24	47.01	39.16	28.22
2 pm	480	48.21	46.23	38.92	27.12
3 pm	540	42.17	44.14	38.63	26.19
4 pm	600	37.12	42.16	37.12	25.12
5 pm	660	36.17	41.83	36.99	25.03
6 pm	720	34.13	40.24	36.73	25.00
7 pm	780	33.16	38.79	35.82	22.28
8 pm	840	32.16	37.16	35.01	21.39
9 pm	900	30.24	36.24	34.74	19.19
10 pm	960	28.17	34.13	32.16	18.24
11 pm	1020	28.02	33.24	30.92	16.79
12midnight	1080	27.11	32.46	29.16	16.23
1 am	1140	26.24	30.24	28.12	12.39
2 am	1200	25.31	28.24	27.11	11.83
3 am	1260	25.03	24.04	25.93	10.28
4 am	1320	24.21	22.01	24.04	9.16
5 am	1380	23.02	21.39	23.72	7.24

Table 2. Predicted daily concentrations of NO_3^- during the wet and dry seasons.

		NO_3^- Concentration ($\mu\text{g}/\text{m}^3$)			
t (min.)		Wet Season 1 st Run	Wet Season 2 nd Run	Dry Season 1 st Run	Dry Season 2 nd Run
6 am	0	20.24	18.26	14.11	12.16
7 am	60	20.01	17.96	13.83	13.79
8 am	120	19.21	17.41	13.01	14.51
9 am	180	18.76	16.92	12.84	14.92
10 am	240	16.23	16.57	12.43	15.33
11 am	300	15.87	16.23	12.32	15.85
12 noon	360	15.25	16.01	12.65	15.67
1 pm	420	14.83	15.86	11.93	15.08
2 pm	480	14.25	15.48	11.46	14.92
3 pm	540	12.96	15.01	10.88	14.84
4 pm	600	11.99	14.87	10.45	14.32
5 pm	660	11.68	14.63	10.21	14.01
6 pm	720	11.15	14.42	9.54	13.74
7 pm	780	11.02	14.03	9.33	13.51
8 pm	840	10.65	13.67	9.03	13.03
9 pm	900	10.24	13.48	8.44	12.73
10 pm	960	10.03	13.04	8.21	12.39
11 pm	1020	10.00	12.75	7.95	11.92
12 midnight	1080	9.95	12.23	7.26	11.74
1 am	1140	9.03	11.46	7.02	10.93
2 am	1200	8.45	11.04	6.84	10.05
3 am	1260	7.96	10.65	6.44	9.62
4 am	1320	6.02	10.00	6.21	8.03
5 am	1380	5.37	9.57	5.97	7.66

Table 3. Predicted daily concentrations of SO_4^{2-} during the wet and dry seasons.

		SO_4^{2-} Concentration ($\mu\text{g}/\text{m}^3$)			
t (min.)		Wet Season 1 st Run	Wet Season 2 nd Run	Dry Season 1 st Run	Dry Season 2 nd Run
6 am	0	32.40	25.28	29.16	34.36
7 am	60	49.16	40.19	53.16	43.17
8 am	120	60.22	49.16	64.22	55.32
9 am	180	84.13	63.16	81.74	69.14
10 am	240	95.67	73.15	91.24	77.32
11 am	300	94.19	77.29	101.99	90.16
12 noon	360	106.32	76.83	111.23	83.73
1 pm	420	95.20	75.16	99.13	80.13
2 pm	480	77.16	59.36	87.14	62.17
3 pm	540	61.24	39.14	62.10	44.16
4 pm	600	48.16	26.65	43.16	42.19
5 pm	660	33.14	21.83	32.17	26.16
6 pm	720	19.15	18.67	19.16	22.43
7 pm	780	14.23	6.95	16.16	16.19
8 pm	840	12.19	5.82	14.28	14.27
9 pm	900	10.72	5.04	12.31	12.39
10 pm	960	9.63	4.48	9.14	11.17
11 pm	1020	7.91	4.29	8.52	9.24
12 midnight	1080	6.99	3.72	7.24	8.67
1 am	1140	5.16	3.21	5.16	6.36
2 am	1200	4.22	2.89	3.46	5.73
3 am	1260	3.86	2.64	2.69	5.02
4 am	1320	3.71	2.23	2.12	3.67
5 am	1380	3.02	1.86	1.86	3.02

Table 4. Predicted daily concentrations of O₃ during the wet and dry seasons.

		O ₃ Concentration ($\mu\text{g}/\text{m}^3$)			
t (min.)		Wet Season 1 st Run	Wet Season 2 nd Run	Dry Season 1 st Run	Dry Season 2 nd Run
6 am	0	7.52	8.28	11.47	14.23
7 am	60	13.49	13.21	15.31	19.16
8 am	120	21.67	20.42	22.95	27.23
9 am	180	27.73	27.19	30.36	35.72
10 am	240	34.81	33.41	35.32	39.16
11 am	300	38.73	38.99	40.70	44.12
12 noon	360	31.78	36.03	37.11	41.25
1 pm	420	33.55	32.03	34.20	38.11
2 pm	480	28.16	27.04	28.55	32.46
3 pm	540	22.48	22.16	24.12	30.13
4 pm	600	17.35	16.17	17.14	21.25
5 pm	660	10.15	10.45	11.75	16.17
6 pm	720	7.62	6.09	7.03	12.12
7 pm	780	2.41	2.98	3.93	8.35
8 pm	840	2.34	2.52	3.21	6.16
9 pm	900	1.99	2.05	2.54	5.25
10 pm	960	1.75	1.72	2.04	4.18
11 pm	1020	1.54	1.67	2.75	3.13
12 midnight	1080	1.49	1.56	2.01	2.56
1 am	1140	1.37	1.53	1.86	2.32
2 am	1200	1.24	1.34	1.63	2.01
3am	1260	1.17	1.24	1.44	1.86
4 am	1320	1.09	1.16	1.21	1.59
5 am	1380	0.73	0.86	0.98	1.43

4. CONCLUSION

PAN, a strong eye irritant, will be felt more in the morning to early afternoon. This secondary pollutant will not be felt as strongly in the period between midnight to early morning. More accumulation of PAN is expected to occur in the morning to early afternoon, causing plant damage. The diurnal behavior of NO₃⁻ concentration is such that it decreases with sunlight and increases with rainfall. Hence the hazes composition of Southeastern Lagos will consist of more PAN and NO₃⁻ in the morning and less of it in the afternoon. In addition, more of these secondary pollutants (PAN and NO₃⁻) will be formed during the wet season when compared with the dry season.

More Ozone and SO_4^{2-} are formed as early afternoon approaches which correspond to maximum concentrations of O_3 and PAN. Hence, photochemical reactions that produced these secondary pollutants (O_3 and SO_4^{2-}) are enhanced with increased sunlight and reduced rainfall. The O_3 and SO_4^{2-} concentrations are higher during the dry season when compared with the wet season

REFERENCES

1. Curtiss P.S., and Rabl A.: Impact Analysis for Air and Water Pollution: Methodology and Software Implementation, in: Zannetti P. (ed.), *Environmental Modeling* – Vol. 3, Computational Mechanics Publications, Southampton, Chapter 13, pp. 393-426, 1996.
2. Dara, S.S.: A Textbook of Engineering Chemistry (revised 10th edition), Chand S and Company Ltd., Ram Nagar, New Delhi, 2006.
3. De More, W.B., Sander, S.P., Golden, D.M., Hampson, R.F., Kurylo, M.J., Howard, C.J., Ravishankara, A.R., Colb, C.E. and Molina, M.J.: Chemical Kinetics and Photochemical Data for Use in Stratospheric Modeling, Eval. 10, pp. 20-92, Jel. Propal. Lab; Pasadena, California, 1992.
4. Froment, G.F. and Bischoff, K.B.: Chemical Reactor Analysis and Design (2nd edition), John Wiley and Sons, New York, 1990.
5. Guyon, P.: Chemical and Physical Properties of Amazonian Aerosol Particles, an unpublished Ph.D. Thesis, University de Paris VII – Denis Diderot, 2002.
6. Hennigan, C.J., Sullivan, A., Fountoukis, C.I., Nenes, A., Hecobian, A., Vargas, O., Peltier, R.E., Caseltants, A.T., Huey, L.G., Lefer, B.L., Russell, A.G. and Weber, R.J.: On the Volatility and Production Mechanisms Of Newly- Formed Nitrate and Water-Soluble Organic Aerosol In Mexico City, *Atmospheric Chemistry and Physics*, 8, pp. 3761-3768, 2008.
7. Henry, J.G. and Heinke, G.W.: Environmental Science and Engineering (2nd Edition), Pearson Education Ltd., Singapore, 2004.
8. Lazaridis, M. and Skouloudis, A.: Computer Simulation of the Transport, Formation and Dynamics of Atmospheric Sulphate Particles, *Water, Air and Soil Pollution*, 112 pp. 171-185, 1999.
9. Massey, B.S.: Mechanics of fluids (2nd edition), Van Nonstrand Reinhold Company, Ltd., London, 2003.
10. Peltier, R.E., Weber, R.J. and Sullivan, A.P.: Investigating a Liquid-based Method for On-line Organic Carbon Detection in Atmospheric Particles, *Aerosol Science and Technology*, 41 pp. 1117-1127, 2007.
11. Pitts, J.N., Winer, A.M., Darnall, K.R., Lloyd, A.C. and Doyle, G.J.: "Proceedings of International Conference on Photochemical Oxidant Pollution and Its Control," Vol. II (B. Dimitriades, ed.), EPA-600/3-77-001b. United States Environmental Protection Agency, Research Triangle Park, N. C. pp. 687-707, 1997.
12. Rao, C.S.: Environmental Pollution Control Engineering (2nd edition), New Age International Publishers, New Delhi, 2006.
13. Sillman and He: Some theoretical Results Concerning O_3 – NO_x – VOC Chemistry and NO_x – VOC Indicators, *Journal of Geophys. Research*, Vol.107, no D22 4659, doi: 10.1029/2001JD001123, 2002.
14. Sonibare, J.A.: A Critical Review of Secondary Pollutants for Gas Flaring, *Journal of Nigerian Society of Chemical Engineers* (In press), 2009a.
15. Stein, A.F. and Lamb, D.: Empirical Evidence for the Low-and High- NO_x Photochemical Regimes of Sphate and Nitrate Formation. *Atmospheric Environment* 37, pp. 3615-3625, 2003.
16. Sullivan, A.P., Weber, R.J., Clement, A.L., Tumer, J.R., Bae, M.S. and Schauer, J.J.: A Method for On-line Measurement of Water-soluble Organic Carbon in Ambient Particles: Results from an Urban Site, *Journal of Geophysical Research Letters*, Vol. 31, L13105, doi: 10.1029/2004GL019681, 2004.
17. Weber, R. J., Marti, J. J. and Mc Murry, P. H.: Measurement of New Particle Formation and Ultrafine Particle Growth Rates at a clean Continental Site, *Journal of Geophysical Research*, vol. 102, No D4, pg 4375 – 4385, 1997.
18. Weber, R.J., Sullivan, A.P., Peltier, R.E., Russell, A., Yan, B., Zheng, M., Degouw, J., Warneke, C., Broch, C., Holloway, J.S., Atlas, E.L. and Edgerton, E.: A Study of Secondary Organic Aerosol Formation in the Anthropogenic-influenced Southeastern United States, *Journal of Geophysical Research*, Vol. 112, D13302, doi: 10.1029/2007JD008408, 2007.
19. Wilson, M.S.: Advance Physical Chemistry, 2nd edition, Galaxy Press Inc., Sydney, Australia, 2004.

MODEL STVARANJA IZMAGLICE KAO POSLEDICE SEKUNDARNIH KONCENTRACIJA ZAGAĐIVAČA U ATMOSFERI

L.A. Jimoda, J.A. Sonibare, F.A. Akeredolu

U ovom radu smo razvili model za predviđanje stope formiranja sekundarnih zagađujućih materija u atmosferi. Zagađivači koji stvaraju izmaglicu, uključujući proizvodnju srednjih perokiacetil nitrata (PAN), ozon (O_3), nitrati (NO_3^-) i sulfat (SO_4^{2-}) su modelirani određivanjem jednačine bilansa za svaku komponentu. Fotohemijski mehanizmi za proizvodnju sekundarnih zagađivača su korišćeni za dobijanje potrebne ravnoteže bi se dobile neophodne jednačine. Početne koncentracije svake komponente u reaktoru i stopa dobijenih konstanti korišćeni su u skupu prvih jednačina za proveru koncentracije (PAN, NO_3^- , SO_4^{2-} , O_3). Šestočasovno uzorkovanja u svakom kvartalu godine je sprovedeno u periodu od 24 sata kako bi se potvrdila koncentracija sekundarnih zagađivača (PAN, NO_3^- , SO_4^{2-} , O_3). Obična diferencijalna jednačina (ODE) Solver programa MATLAB 8.0 je korišćena za određivanje profila koncentraciju sekundarnih zagađivača svakog sata tokom 24 časa. Rezultati su pokazali da su se koncentracije perokiacetil nitrat (PAN) i NO_3^- smanjile sa sunčevim zracima ali povećale sa padavinama, dok su se koncentracije ozona (O_3) i sulfata (SO_4^{2-}) povećale sa sunčevim zracima a smanjile i sa padavinama. Rezultati dobijeno od razvijenog rezultati potvrdili su varijacije u koncentracijama sekundarnih zagađivača u odnosu na sunce i padavine.

Ključne reči: stvaranje izmaglice, sekundarni zagađivači, fotohemijske reakcije, lančana reakcija